

Dissipation and strain-stiffening behavior of pectin-Ca gels, under LAOS (Supporting Information)

Jacob John,[†] Debes Ray,[‡] Vinod K. Aswal,[‡] Abhijit P. Deshpande,[†] and Susy
Varughese^{*,†}

[†]*Department of Chemical Engineering, Indian Institute of Technology, Madras, India*

[‡]*Solid State Physics Division, Bhabha Atomic Research Centre, Mumbai, India*

E-mail: susy@iitm.ac.in

0.1 Details of the SANS experiments

The scattering profiles of the gel samples were measured after packing them in aluminium foils which are fairly transparent to neutrons. Care has been taken during packing to ensure that the gel is bubble-free. The sample thickness was 2 mm, and the scattered intensity from the sample was corrected for sample holder (aluminium foil) as well as sample thickness. The data was analyzed by comparing the scattering from different models to the experimental data.

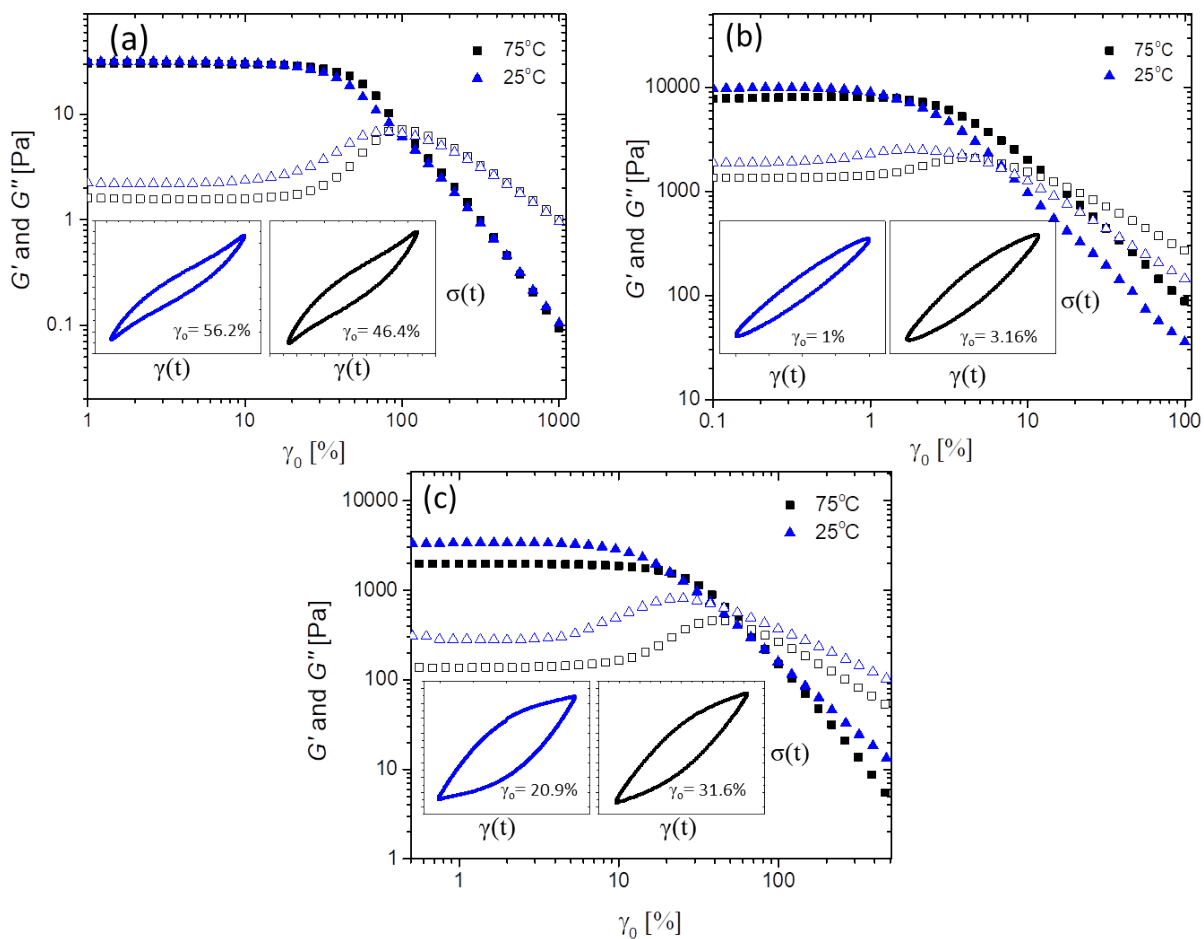


Figure S1: The variation of G' (closed symbols) and G'' (open symbols) with strain amplitude for gels prepared at 25 °C (blue symbols) and 75 °C (black symbols). The composition of the gels are as follows (a) $R=0.5$ and $c=1$ wt%, (b) $R=3$ and $c=1$ wt% and (c) $R=0.5$ and $c=2.5$ wt%. The intra-cycle stress vs strain data at a representative strain amplitude in the ‘region-2’ (mentioned in the main article) is shown in the insets of each of the figures.

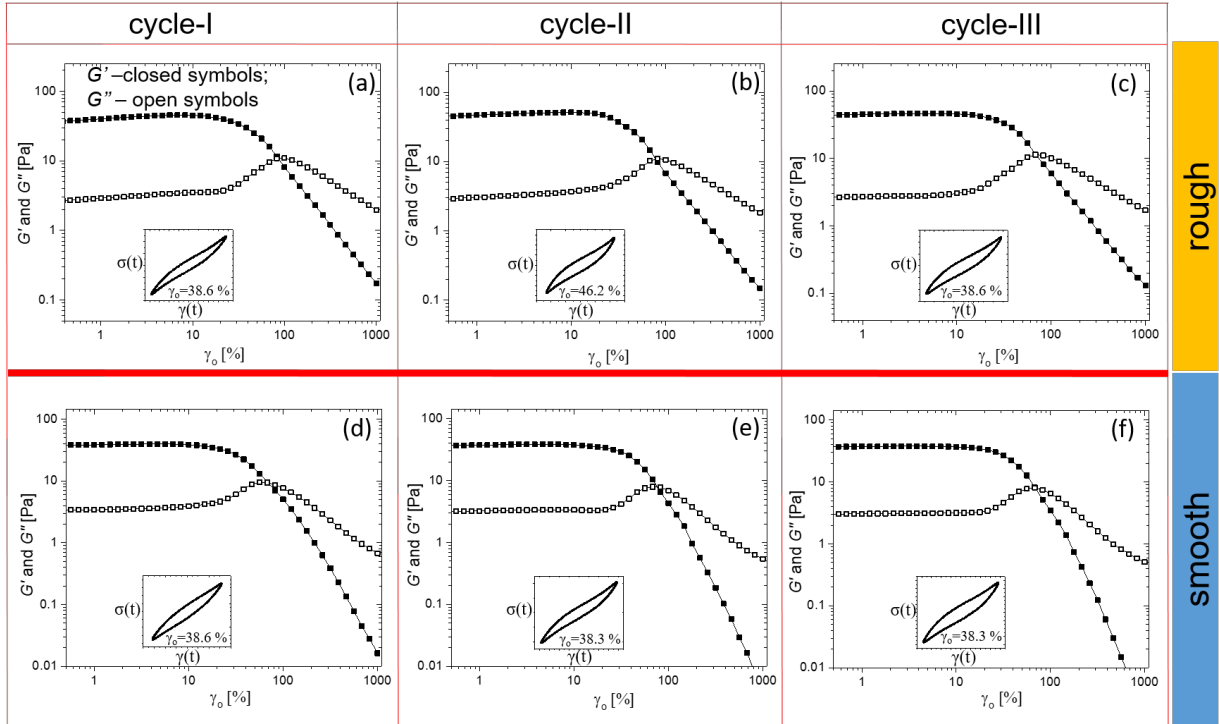


Figure S2: The variation of G' (closed symbols) and G'' (open symbols) with strain amplitude for gels at $c=1$ wt% and $R=0.5$ during multiple cycles of strain sweeps performed using smooth and rough geometries, at a frequency of 1 Hz. (a), (b) and (c) correspond to cycles I, II and III performed in a rough geometry, while, (d), (e) and (f) correspond to cycles I, II and III performed in a smooth geometry. The insets show the Lissajous plots at a strain amplitude in region-2 (Figure 4).

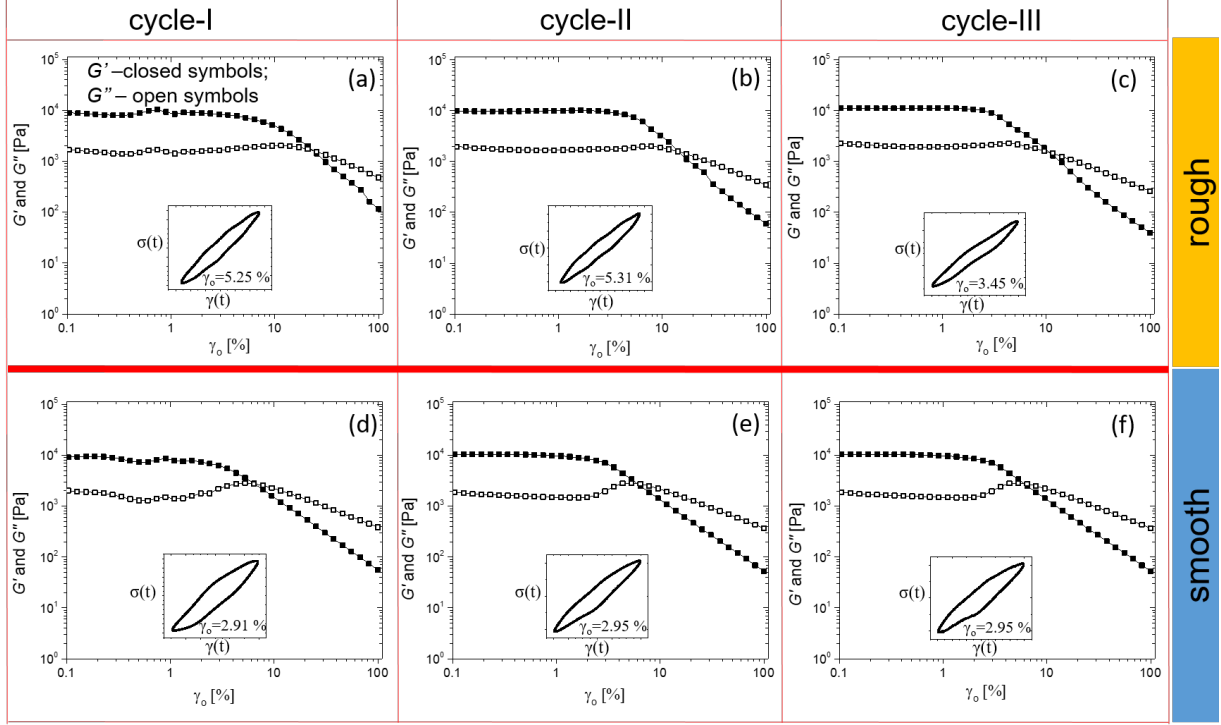


Figure S3: The variation of G' (closed symbols) and G'' (open symbols) with strain amplitude for gels with $c=1$ wt% and $R=3$ during multiple cycles of strain sweeps performed using smooth and rough geometries, at a frequency of 1 Hz. (a), (b) and (c) correspond to cycles I, II and III performed in a rough geometry, while, (d), (e) and (f) correspond to cycles I, II and III performed in a smooth geometry. The insets show the Lissajous plots at a strain amplitude in region-2 (Figure 5).

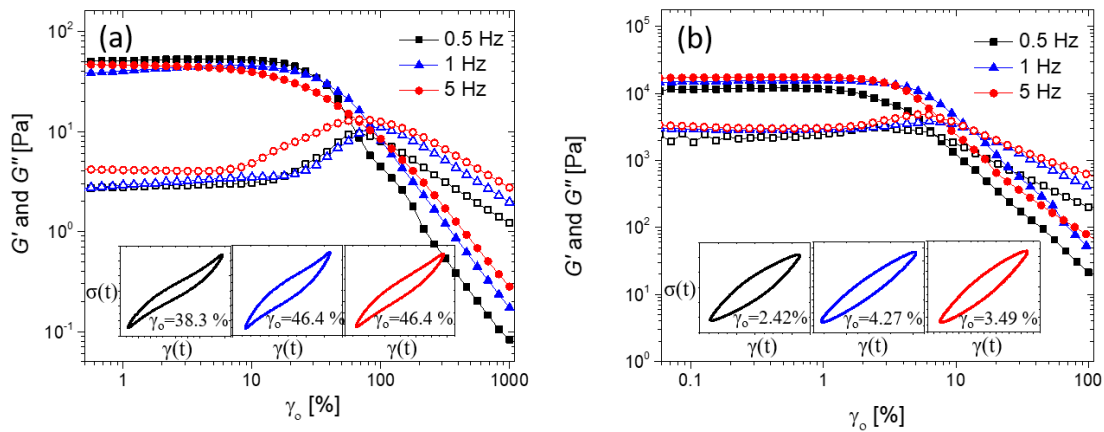


Figure S4: The variation of G' (closed symbols) and G'' (open symbols) with strain amplitude for gels with $c=1$ wt% and (a) $R=0.5$ and (b) $R=3$, at different frequencies of deformation. The insets show the intra-cycle stress-strain data at a representative strain amplitude in region-2 (Figures 4 and 5, main article) at different frequencies.

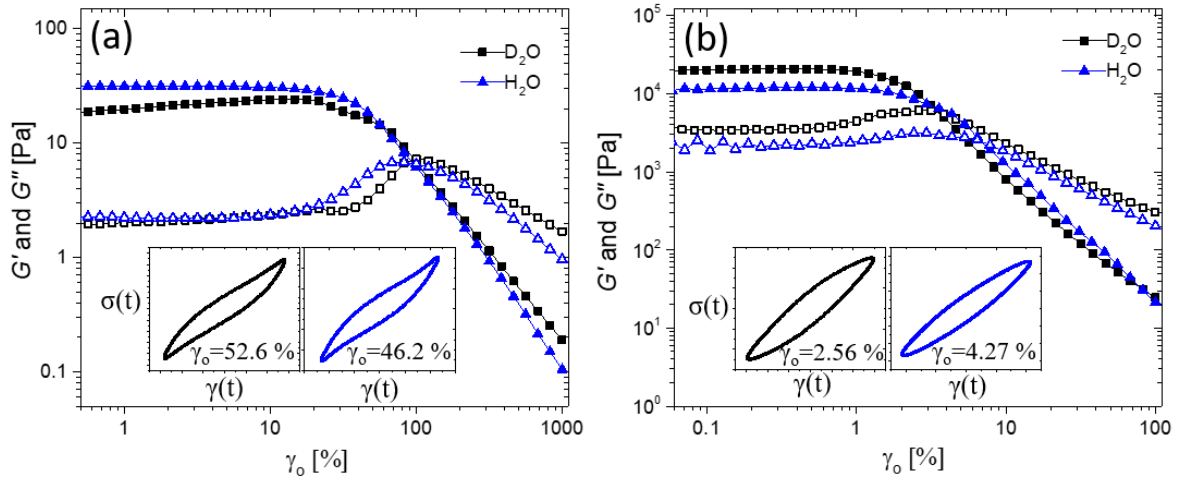


Figure S5: The variation of G' (closed symbols) and G'' (open symbols) with strain amplitude for gels prepared in D_2O (black symbols) and H_2O (blue symbols), with $c=1$ wt% and (a) $R=0.5$ and (b) $R=3$, at a frequency of 1 Hz. The insets show the intra-cycle stress-strain data at a representative strain amplitude in region-2 (Figures 4 and 5, main article).

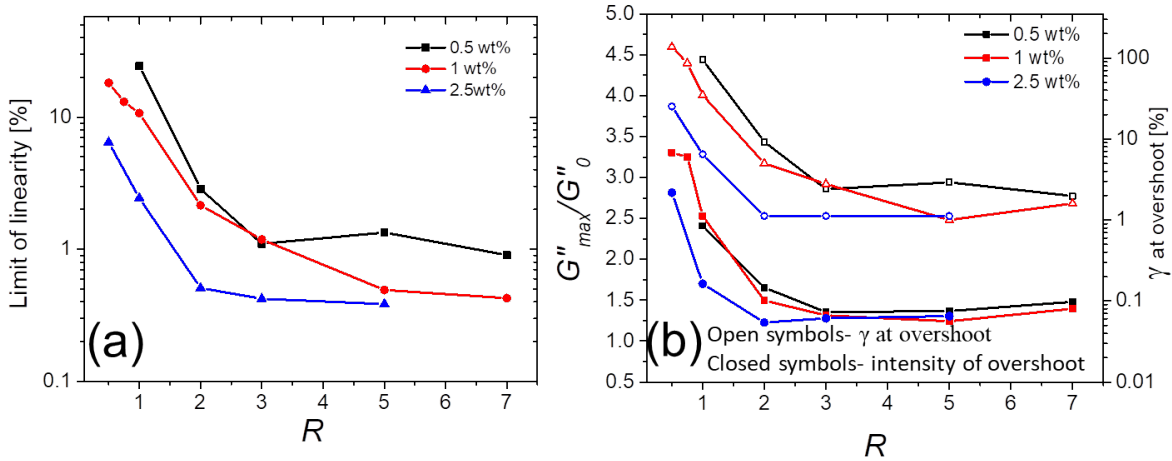


Figure S6: Variation of (a) limit of linearity and (b) intensity and position of G'' overshoot, as a function of R , at different pectin concentrations, c .

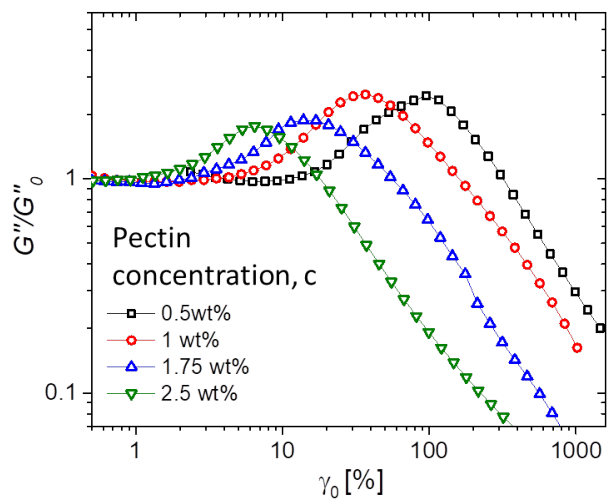


Figure S7: Variation of normalized G'' with shear strain amplitude, at different pectin concentrations, c , at $R=1$.

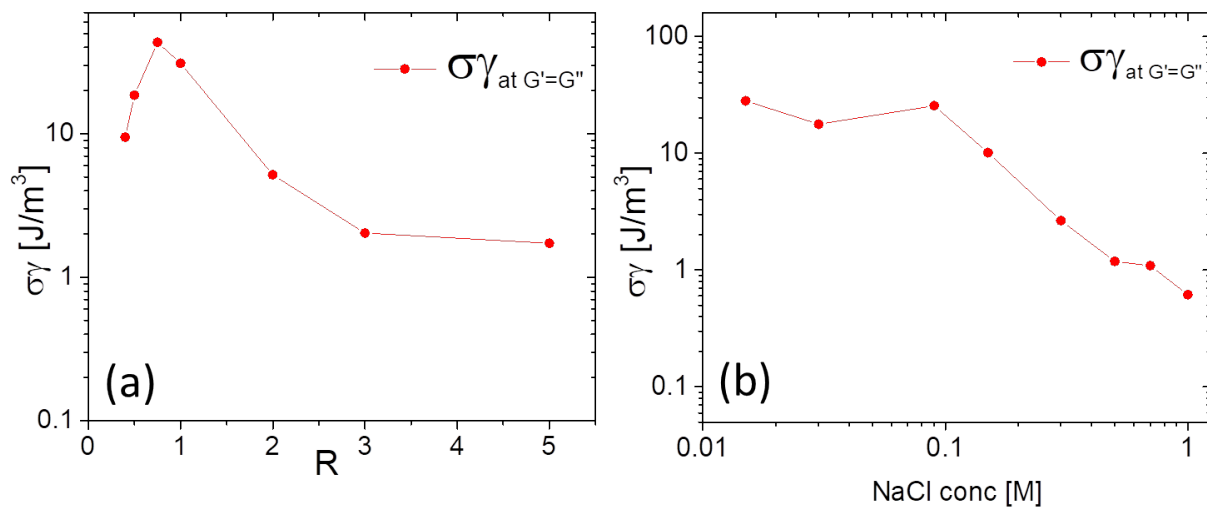


Figure S8: The energy associated with the strain amplitude at which the cross-over of G' and G'' occur as function of (a) R , for $c=1$ wt% and (b) NaCl concentration, for $R=0.5$ and $c=1$ wt%.

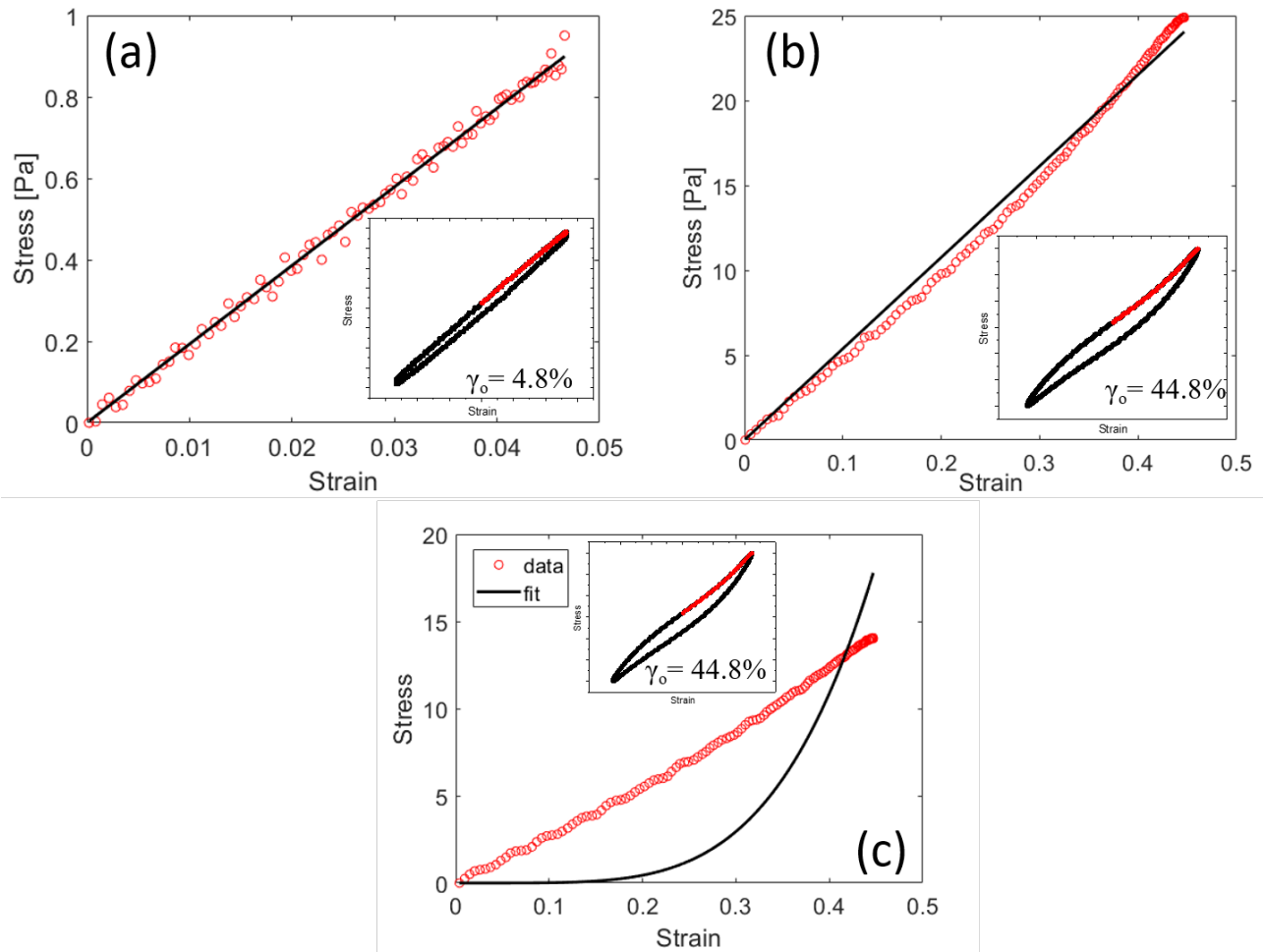


Figure S9: (a) Stress-strain data in the first quarter of the Lissajous plot, and fit (continuous black line) to the data using Equation-2 (main article) at a strain amplitude of (a) 4.8% (region-1, Figure 4) and (b) 44.8% (region-2, Figure 4, main article). (c) fit to the data using the Equation-3 at a strain amplitude of 44.8% (region-2, Figure 4).

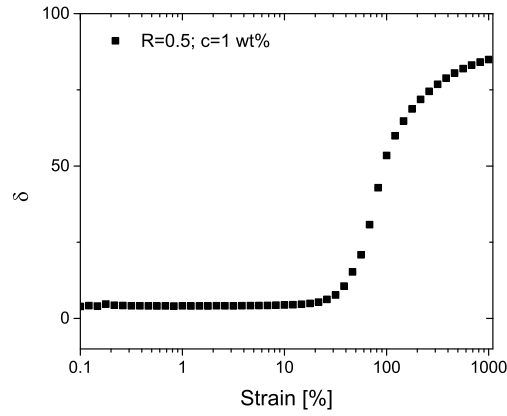


Figure S10: Variation of phase angle as a function of shear strain amplitude for pectin-Ca gel with $R=0.5$ and $c=1$ wt%.

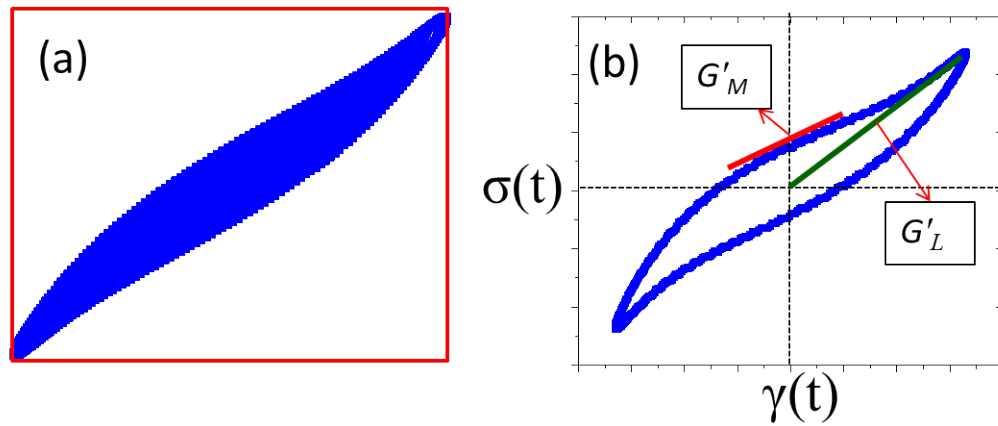


Figure S11: (a) The calculation of dissipation coefficient (Ψ)- ratio of the area enclosed within the Lissajous curve (blue shaded region) to that of the rectangle (red) (b) slopes G'_L and G'_M used in equation 7.

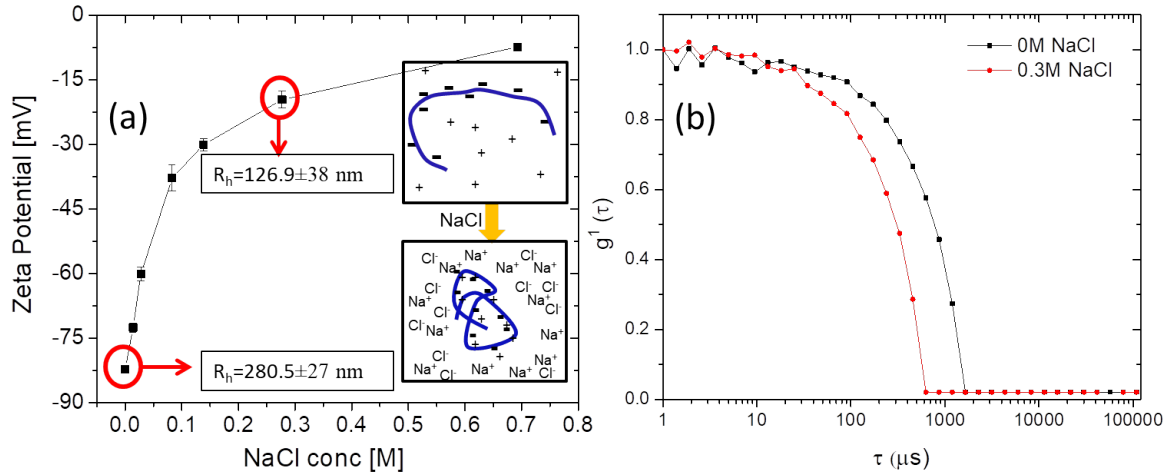


Figure S12: (a) The variation of zeta potential of pectin solution with NaCl concentration. (b) Hydrodynamic radius measured using dynamic light scattering (at $c=0.05$ wt%) is shown for the case of no salt and 0.3 M NaCl.

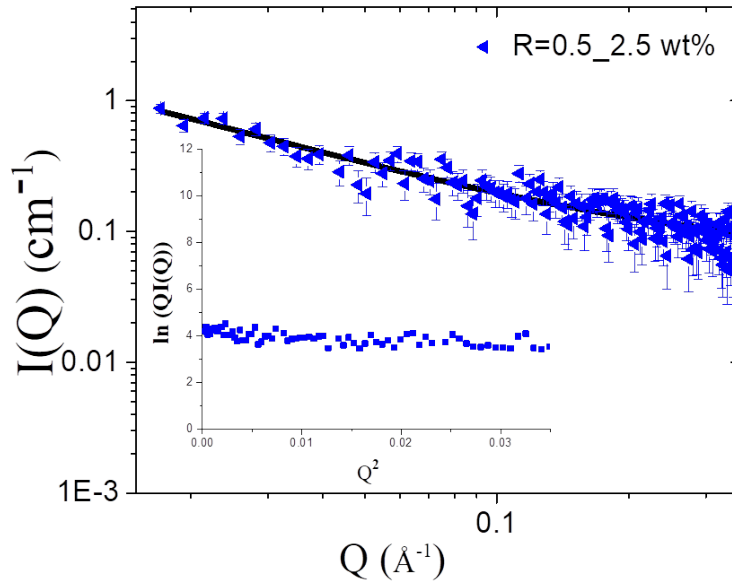


Figure S13: SANS profiles for pectin-Ca gels prepared at $c = 2.5$ wt% ($c > c^{**}$), at $R=0.5$. Insert shows the Guinier plot for the same gel. Fisher-Burford model fitting as well as the Guinier analysis resulted in a fractal dimension of 1.35 ± 0.08 , R_g value of 81.6 ± 10 \AA and Guinier radius of 5.74 ± 0.72 \AA .

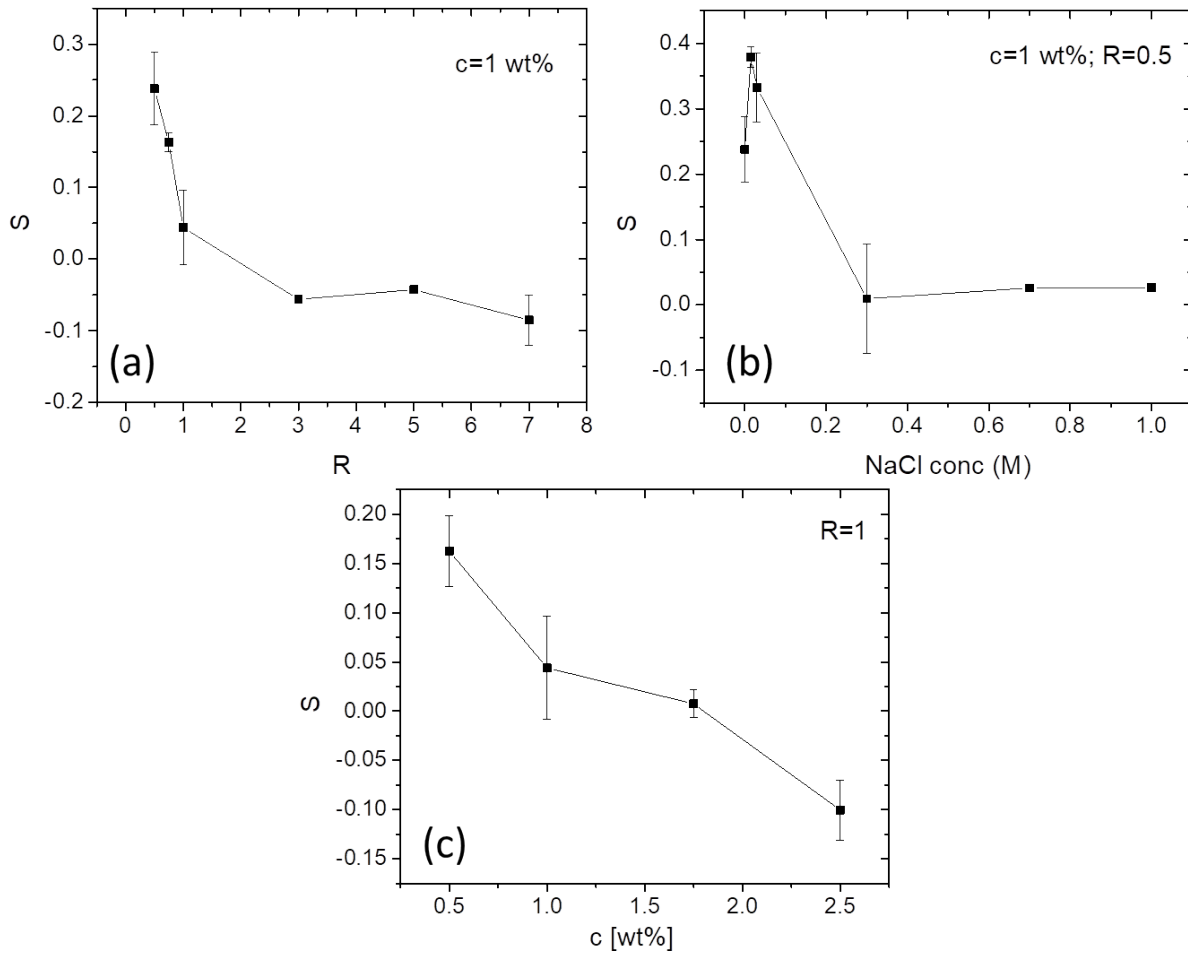


Figure S14: Samples that show intracycle strain stiffening at strain amplitudes in 'region-2' have a positive value for the strain stiffening index 'S'. The variation of 'S' with (a) R , at $c=1$ wt%, (b) NaCl concentration at $R=0.5$; $c=1$ wt% and (c) c , at $R=1$.

Table 1: Summary of the analysis using the strain stiffening model (sum of equations 2 and 3, main article) for pectin-Ca gels of various compositions that show a strain-stiffening response. The strain amplitude (γ_0) in the 'region-2', at which the intracycle data is used for the fitting, as well as the 'k' and 'G' values obtained from the fitting are tabulated against the compositions of the gels. Non-negative values for 'k' were obtained only for the strain-stiffening gels. The 'G' values obtained from the fit were comparable to the experimentally observed G'_M and G' values of the corresponding gels, at the strain amplitudes mentioned.

R	NaCl conc (M)	c wt%	'k' (Pa)	G (Pa)	γ_0 (%)
0.5	0	1	11.96 ± 0.8	27.65 ± 0.13	44.6
0.75	0	1	$16.4 \pm 1.$	116.87 ± 15.6	36.3
0.5	0.015	1	11.21 ± 1.33	45.2 ± 7.73	54.6
0.5	0.03	1	11.69 ± 0.53	59.61 ± 2.72	44.6
0.5	0.09	1	10.29 ± 1.71	66.76 ± 7.35	36.2
0.5	0	0.5	7.77 ± 1.15	7.73 ± 0.97	64.2

Table 2: Summary of the analysis using the Dobrynin model (Equation-4) for pectin-Ca gels of various compositions that show a strain-stiffening response in 'region-2'. The strain amplitude(γ_0) in the 'region-2', at which the intracycle data is used for the fitting, as well as the ' K ' and ' β ' values obtained from the fitting are tabulated against the compositions mentioned.

R	NaCl conc (M)	c wt%	β	K	γ_0 (%)
0.5	0	1	0.73	1191.2	44.6
0.75	0	1	0.67	1562.9	36.3
0.5	0.015	1	0.74	1944.9	54.6
0.5	0.03	1	0.72	1586.8	44.6
0.5	0.09	1	0.73	2193.2	36.2